Indian J. Genet. Plant Breed., (2025); 85(2): 280-289
https://doi.org/10.31742/ISGPB.85.2.13
ISSN: 0975-6906
www.isgpb.org

RESEARCH ARTICLE

A comprehensive transcriptome analysis reveals the key mechanism related to leaf colour variation in a xantha mutant of *Cucumis melo* L.

Qin Shao[$*], Wenjun Zhang, Xin Zhong, Na Chen[1], Liangliang Liu[2], Weihai Yang[1] and Xiaopeng Li[1]

Abstract

This study aimed to investigate the key mechanisms underlying variation in leaf colour in the xantha mutant of *Cucumis melo*. The normal green *C. melo* inbred line 'Baishami NO.1' (wild type) and its spontaneous mutant' 9388-1' (xantha mutant) were collected. A comprehensive transcriptome analysis was conducted to identify differentially expressed genes (DEGs) between wild-type and xantha mutant *C. melo* in both the cotyledon and euphylla stages. A functional enrichment analysis, transcription factor (TF) prediction and a protein-protein interaction (PPI) network analysis for differentially expressed genes (DEGs) were subsequently conducted. In total, 234 up- and 551 down-regulated common DEGs in both the cotyledon and euphylla stages of xantha mutant *C. melo* were identified. These DEGs were significantly enriched in functions or pathways associated with photosynthesis and chloroplast development. Moreover, 18 common DEGs were identified as TFs that belonged to the ERF family. Notably, the photosynthesis-related gene MELO3C010813 (*ZAT10*) that was identified was also found to be a TF that belongs to the ethylene response factor family. A PPI network analysis showed that MELO3C023986 had the highest with *TOP2* in *Arabidopsis thaliana*, and our findings revealed that expression of the xantha mutant phenotype may be associated with the abnormal expression of *ZAT10*, *MAPK3*, *CRD1*, *PORA* and *ERF* TFs, as well as the dysregulation of photosynthesis and chloroplast development.

Keywords: Differentially expressed genes, functional enrichment analysis, PPI network, RNA-seq, TF prediction.

Introduction

Leaf-colour mutants commonly occur among in higher plants, and they have been identified in a wide variety of crops, including rice (*Oryza sativa*) (Deng et al. 2017; Chen et al. 2018), maize (*Zea mays*) (Yang et al. 2012; Yuan et al. 2021), wheat (*Triticum aestivum* L.) (Wu et al. 2018) and strawberry (Fragaria×ananassa Duch.) (Peng et al. 2025).

Chlorophylls, carotenoids and anthocyanins are the main pigment classes that affect the formation of leaf colour. A defect in the metabolism of photosynthetic pigments is considered to be a common cause of leaf-colour mutant phenotypes (Ma et al. 2017; Huang et al. 2024). Hu et al. (2007) revealed that the ratio of chlorophyll/carotenoids, as well as the contents of chlorophyll, in golden leaves increase as the position of leaf becomes lower on the plant. In addition, chlorophyll is the primary photosynthetic pigment, responsible for harvesting solar energy in the antenna systems and driving electron transport in the reaction centers (Tanaka and Tanaka, 2006; Wang et al. 2024). Furthermore, an additional transcriptome profiling analysis revealed that the expression of some unigenes that belong to the chlorophyll A/B binding protein (*CAB*) and golden

College of Life Science and Environmental Resources, Yichun University, Yichun 336000, China.

[$]Present address and [1]Key Laboratory of Controlling and Regulating of Crop Growth and Development of Jiangxi Province, Yichun University, Yichun, 336000, China.

[2]Engineering Technology Research Center of Jiangxi Universities and Colleges for Selenium Agriculture, Yichun University, Yichun 336000, China.

***Corresponding Author:** Qin Shao, College of Life Science and Environmental Resources, Yichun University, Yichun 336000, China, E-Mail: shaoqin2013@126.com

How to cite this article: Shao Q., Zhang W., Zhong X., Chen N., Liu L., Yang W. and Li X. 2025. A comprehensive transcriptome analysis reveals the key mechanism related to leaf colour variation in a xantha mutant of *Cucumis melo* L. Indian J. Genet. Plang Breed., **85**(2): 280-289.

Source of support: National Natural Science Foundation of China (32160716, 32260776)

Conflict of interest: None.

Received: Oct. 2024 **Revised:** March 2025 **Accepted:** April 2025

© The Author(s). 2025 Open Access This article is published by the Indian Society of Genetics & Plant Breeding, NASC Complex, IARI P.O., Pusa Campus, New Delhi 110 012; Online management by www.isgpb.orgw

Fig. 1. Phenotypes of the plant materials. (A) Cotyledon of the wild type 'Baishami NO.1' (B) Cotyledon of the xantha mutant' 9388-1'; (C) Seedling of 'Baishami NO.1' and '9388-1'; (D) flowering period of '9388-1';(E)flowering and fruiting period of 'Baishami NO.1' and '9388-1'

2-like (*GLK*) gene families are associated with chloroplast development, and these genes may affect leaf colour via the regulation of chloroplast biogenesis and development, and chlorophyll metabolism, and subsequent reduction in the content of chlorophyll and photosynthetic capacity (Li et al. 2015; Fang et al. 2024). Previous studies indicated that the leaf colour yellowing phenotype of cucumber mutant' 9388-1' might have been caused by chloroplast development defects (Shao and Yu 2013). Nevertheless, the molecular mechanism that underlies the formation of leaf colour mutant phenotypes remains largely unknown.

To discover candidate genes related to leaf colour in xantha mutant *C. melo*, we performed a comprehensive transcriptome analysis to identify differentially expressed genes (DEGs) between wild-type and xantha mutant *C. melo* in both the cotyledon and euphylla stages. A functional enrichment analysis, transcription factor (TF) prediction and protein-protein interaction (PPI) network analysis were subsequently conducted. The results of this study will facilitate a better understanding of the mechanisms underlying mutant phenotypes, enabling a deeper understanding of photosynthetic and physiological processes in plants.

Materials and methods

Plant material

The standard green *C. melo* inbred line 'Baishami NO. 1' was used as the wild-type (WT) background. The spontaneous mutant' 9388-1' was used as the xantha mutant (Fig. 1). All *C. melo* plants were grown in a Phytotron at 28/20°C (day/night) under a 16h illumination time with a light density of 25,000 Lux. The cotyledons (T01 and T02) and the euphyllas (T03 and T04) of the WT and xantha *C. melo* were then collected. Biological replicates were performed three times, respectively.

RNA isolation, cDNA library construction and sequencing

Total RNA was extracted from the cotyledon and euphylla of the WT and xantha mutant lines of *C. melo* using an RNAiso Plus Kit (TaKaRa Bio Inc., Shiga, Japan). The purity, concentration and integrity of each RNA sample were detected using a NanoDrop spectrophotometer (Nanodrop Technologies, Waltham, MA, USA), a Qubit 2.0 fluorometer (Life Technologies Group, Carlsbad, CA, USA), and an Agilent 2100 bioanalyzer (Agilent Technologies, Santa Clara, CA, USA), respectively. The mRNA was isolated from the total RNA using oligo (dT) magnetic beads and then cleaved into short fragments as templates for the synthesis of first-strand cDNA based on random hexamer primers. Subsequently, double-stranded cDNA was synthesized and subjected to end repair, dA tailing and adaptor ligation. The products were then size-selected using AMPure XP beads (Agencourt Bioscience Corporation, Beverly, MA, USA) and enriched by PCR to construct the cDNA library. The established cDNA libraries were then quantified and validated using a Qubit 2.0 fluorometer and Agilent 2100 bioanalyzer, followed by sequencing on an Illumina HiSeqTM 2500 platform (Illumina, Inc., San Diego, CA, USA) using 125 bp paired-end reads.

Quality control, read mapping, transcriptome assembly and annotation

Quality control for the raw reads was performed to remove adapter sequences and low-quality reads, thereby obtaining clean reads. The clean reads were subsequently aligned to the reference *C. melo* genome (https://melonomics.net/files/Genome/Melon_genome_v3. 5.1/) to obtain mapped reads using TopHat 2v. 2.1.1 (Kim et al. 2013), followed by the calculation of the read mapped ratio, defined as the ratio of the number of mapped reads to the number of clean reads. The mapped reads were then assembled using the Cufflinks package (release 0.8.2) (http://cufflinks.cbcb.umd.edu/) (Trapnell et al. 2010). Gene function annotation was then conducted using BLAST software searches against the *C. melo* database (Altschul et al. 1997). To calculate gene expression level, the number of mapped reads and the length of transcripts were homogenized based on fragments per kilo-base of transcript per million fragments mapped (FPKM), as calculated using the Cufflinks package.

DEGs selection

The DEGs in the T02 vs T01 comparison, as well as the T04 vs T03 comparison, were identified, respectively, using EBSeq (Leng et al. 2013). The *P* value threshold for differential expression was adjusted according to the false discovery rate (FDR) using the Benjamini and Hochberg (BH) method (Benjamini and Hochberg 1995). The genes with values of FDR <0.01 and |log2 fold change (FC)| ≥1 were considered

to be DEGs. To mine the DEGs that had the same changes in expression in the T02 vs T01 and T04 vs T03 comparisons, we constructed Venn diagrams using VennPlex software (http://www.irp.nia.nih.gov/bioinformatics/vennplex.html) to identify common DEGs (Cai et al. 2013).

Functional annotation, enrichment analysis and TF prediction

To better understand the function of DEGs, the DEGs identified in different groups were then subjected to Gene Ontology (GO, http://www.geneontology.org/) function and Kyoto Encyclopedia of Genes and Genomes (KEGG, http://www.genome.jp/kegg/) pathway enrichment analyses using Cluster Profiler (Yu et al. 2012). The threshold value was established as $p < 0.05$. As TFs are involved in plant growth and development, the TFs among the common DEGs were also predicted using the Plant Transcription Factor Database *(plant TFDB*).

Construction of the PPI network

The PPI pairs of common DEGs were extracted from STRING version 10.5 (Szklarczyk et al. 2017) (http://string-db.org/). Because no data corresponded to *C. melo* in the STRING database, soybean (Glycine max), which has a genome sequence with high homology to that of *C. melo* and a relatively closer homologous relationship, was selected for analysis. Briefly, we downloaded protein sequences of soybean from the STRING database and then used them for BLAST analysis against *C. melo* proteins to infer the corresponding relationship of genes between these two species. The PPI pairs between genes were then predicted with Required Confidence (combined score) > 0.5. Subsequently, the PPI network was constructed using Cytoscape version 3.6.0 (Shannon et al. 2003) (http://www.gene names.org/). The hub node was then identified by calculating the degree score. A higher degree score indicates a more important location in the network.

Results and discussion

Quality control and read mapping

After quality control to filter out the adapter sequences and low-quality reads, a total of 33.59 Gb clean data were obtained, and the percentage of base calls greater than Q30 for T01, T02, T03 and T04 were 85.32, 86.03, 85.89, and 86.50%, respectively. In addition, after mapping reads to the reference genome of *C. melo,* the mapped read rates of all the samples were as high as 86.42%, and the unique mapped rates were greater than 84.60% (Table 1).

DEG analysis

Gene expression levels were calculated as FPKM values. For cut-off values of FDR <0.01 and |log2 FC| ≥1, 1,165 up- and 1,661 down-regulated genes were identified in the T02 vs T01 comparison, respectively, and 812 up- and 1,774 down-regulated genes were identified in the T04 vs T03 comparison, respectively. Furthermore, the Venn diagram showed that there were 234 up- and 551 down-regulated common DEGs in both the T02 vs T01 and T04 vs T03 comparisons (Fig. 2).

Functional enrichment analysis

The significantly enriched top 10 GO terms among biological process (BP), cellular component (CC) and molecular function (MF) terms are displayed in Figs. 3, 4 and 5, respectively. In detail, the DEGs identified from the T02 vs T01 comparison were significantly enriched in GO BP terms associated with response to GO:1901700: oxygen-containing compound, GO:0072330: monocarboxylic acid biosynthetic process, and GO:0009765: photosynthesis, light harvesting; GO CC terms related to GO:0009536: plastid, GO: 0009507: chloroplast, and GO:0009534: chloroplast thylakoid; GO MF terms associated with GO:0016491: oxidoreductase activity,

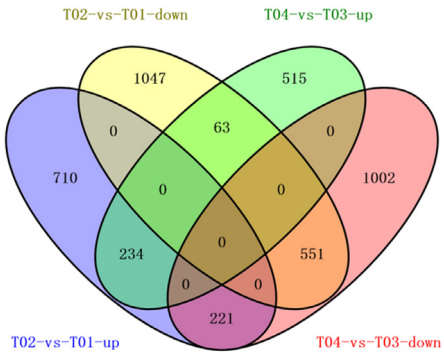

Fig. 2. Venn diagram of differentially expressed genes between wide type and xantha mutant of Cucumis melo in both cotyledon and euphylla stages. The cotyledon (T01 and T02) and the euphylla (T03 and T04) of the wild type and xantha of C. melo were respectively collected.

Table 1. The transcriptome sequencing data statistics of all C. melo sample

Sample ID	Total reads	Base Number	%≥Q30	Mapped reads	Mapped ratio	Unique mapped reads	Unique mapped ratio
T01	67,532,718	8,505,574,224	85.32%	58,360,309	86.42%	57,135,785	84.60%
T02	70,260,826	8,847,795,670	86.03%	61,255,154	87.18%	60,018,378	85.42%
T03	59,832,708	7,534,935,906	85.89%	52,447,909	87.66%	51,667,243	86.35%
T04	69,126,336	8,705,241,063	86.50%	60,481,079	87.49%	59,883,511	86.63%

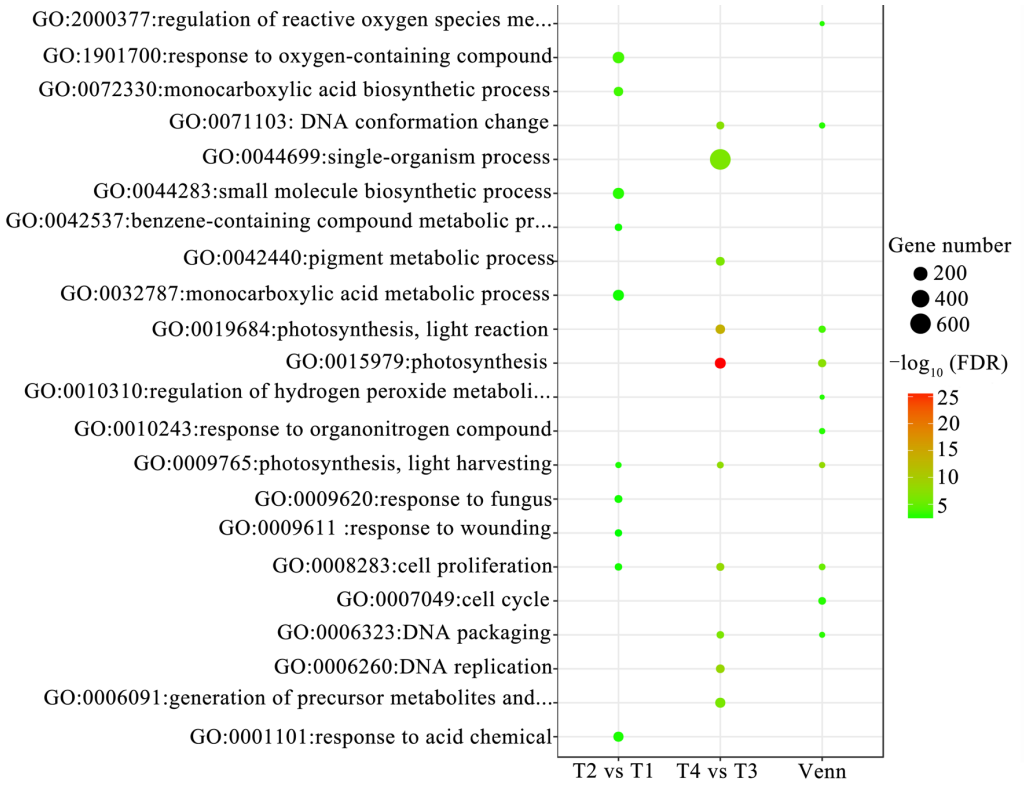

Fig. 3. The top 10 GO terms in biological process (BP) enriched by differentially expressed genes identified from T02 vs T01 comparison, T04 vs T03 group, and both T02 vsT01 and T04 vs T03 comparison.

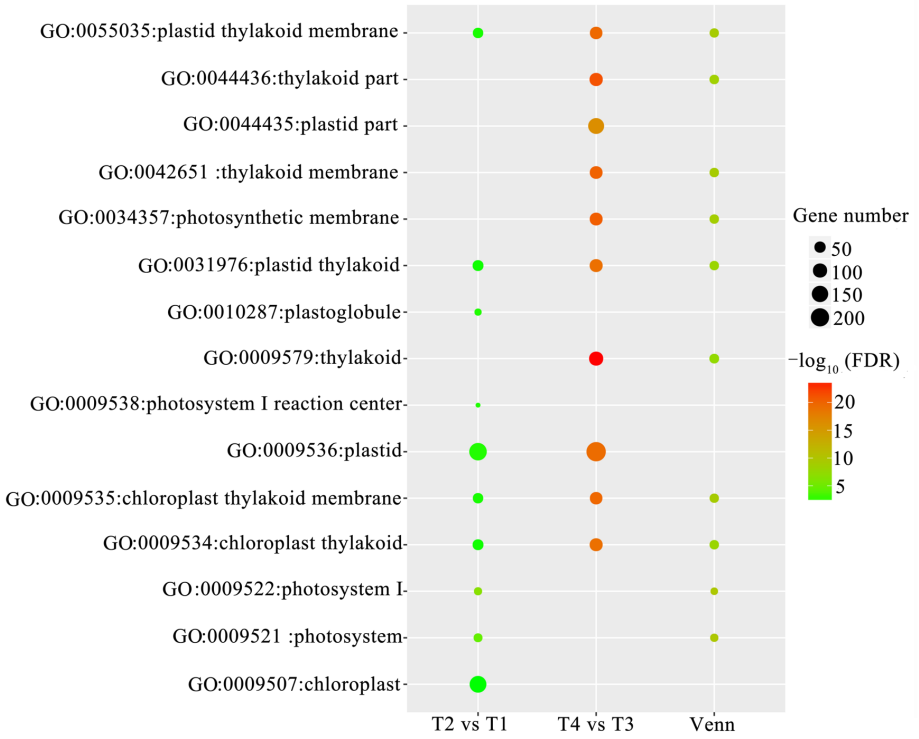

Fig. 4. The top 10 GO terms in cellular component (CC) enriched by differentially expressed genes identified from T02 vs T01 comparison, T04 vs T03 comparison, and both T02 vs T01 and T04 vs T03 comparison

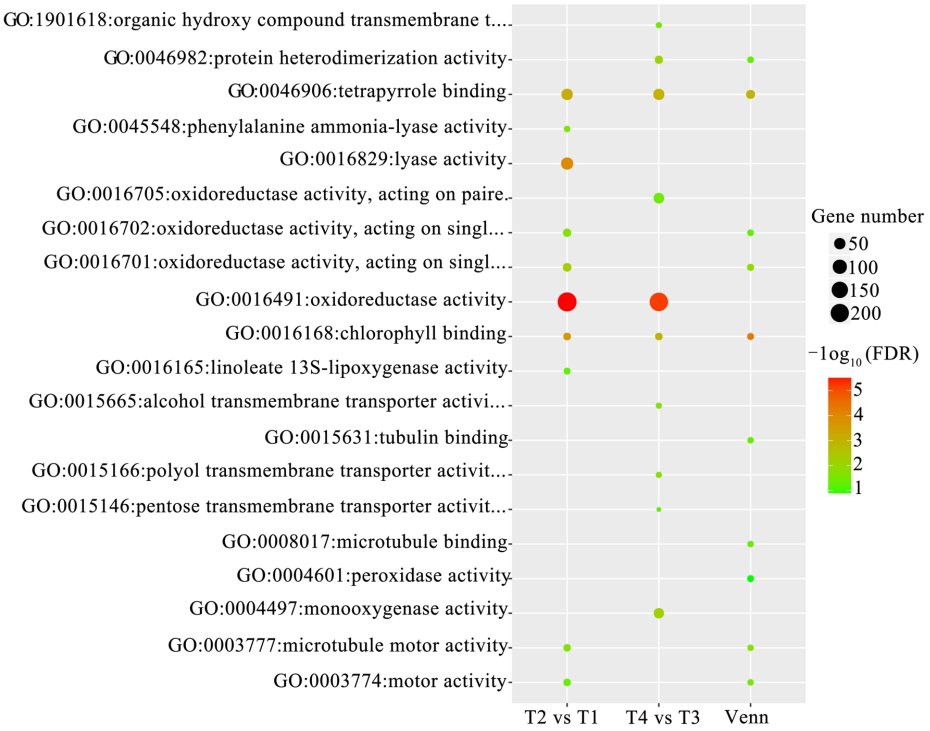

Fig. 5. The top 20 GO terms in molecular function (MF) enriched by differentially expressed genes identified from T02 vs T01 comparison, T04 vs T03 comparison, and both T02 vs T01 and T04 vs T03 comparison.

GO:0046906: tetrapyrrole binding, and GO:0016829: lyase activity.

The DEGs identified from the T04 vs T03 comparison were remarkably enriched in GO BP terms closely related to GO:0044699: single-organism process, GO:0015979: photosynthesis, and GO:0009765: photosynthesis, light harvesting; GO CC terms associated with GO:0009536: plastid, GO:0009579: thylakoid, and GO:0034357: photosynthetic membrane; GO MF terms associated with GO:0016491: oxidoreductase activity, GO:0004497: monooxygenase activity, and GO:0046906: tetrapyrrole binding.

The common DEGs identified from both the T02 vs T01 and T04 vs T03 groups had GO BP terms relatively significantly enriched in GO:0015979: photosynthesis, GO:0019684: photosynthesis, light reaction, and GO:0009765: photosynthesis, light harvesting; GO CC terms associated with GO:0055035: plastid thylakoid membrane, GO:0031976: plastid thylakoid, GO:0009534: chloroplast thylakoid, and GO:0009535: chloroplast thylakoid membrane; GO MF terms connected with GO:0046906: tetrapyrrole binding, GO:0016168: chlorophyll-binding, and GO:0004601: peroxidase activity.

Notably, based on the enriched GO functions, key DEGs associated with photosynthesis were identified, such as MELO3C010813 (zinc finger protein *ZAT10*) and MELO3C020718 (mitogen-activated protein kinase 3, *MAPK3*), and some DEGs associated with the chloroplast were also identified, including MELO3C026802 (cyclase, chloroplastic (Precursor), *CRD1*) and MELO3C016714 (protochlorophyllide reductase, chloroplastic (Precursor), *PORA*).

Furthermore, the top 10 KEGG pathways enriched by the DEGs in each comparison are also shown in Fig. 6, which shows the overrepresented KEGG pathways enriched by DEGs identified from the T02 vs T01 and T04 vs T03 comparisons, both of which include ko00195: photosynthesis, ko00196: photosynthesis antenna proteins, and ko04075: plant hormone signal transduction.

TF prediction analysis

To better understand the function of common differentially expressed genes (DEGs) in plant growth and development, the transcription factors (TFs) that shared these DEGs were predicted. Eighteen shared DEGs were TFs, which belonged to 11 TF families (Table 2). Notably, MELO3C005502, MELO3C005867, MELO3C006430, MELO3C012896, and MELO3C017940, which all belong to the ERF family, were identified. In addition, the photosynthesis-related gene MELO3C010813 was also identified as a TF, and it belongs to the ethylene response factor family.

PPI analysis

Based on the STRING database, the PPI network constructed using common differentially expressed genes (DEGs)

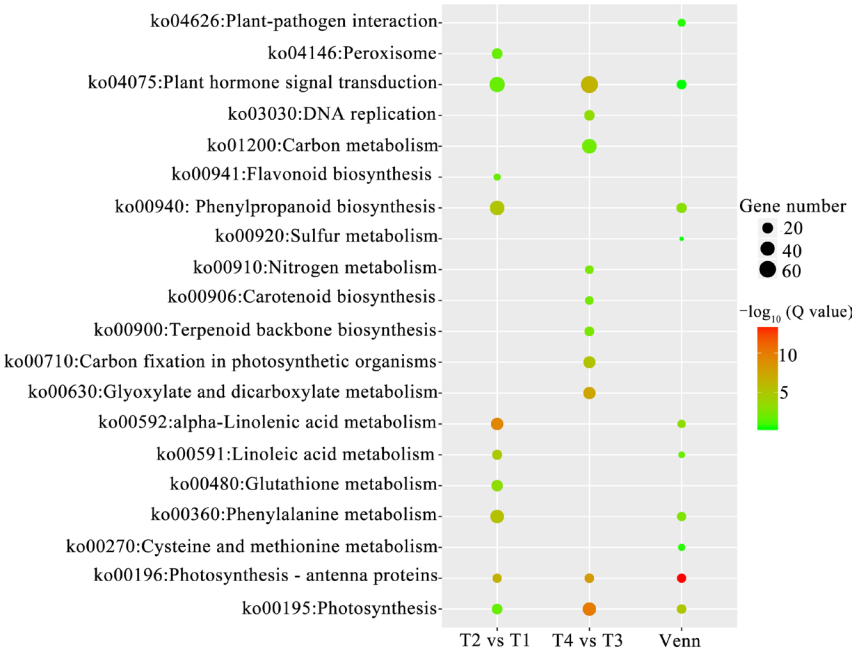

Fig. 6. The top 10 KEGG pathways enriched by differentially expressed genes identified from T02 vs T01 comparison, T04 vs T03 comparison, and both T02 vs T01 and T04 vsT03 comparison

contained 275 nodes and 1,330 edges (Supplementary Fig. 1). After calculating the degree score, the top 10 hub nodes in the PPI network were identified, including MELO3C023986 (up-regulated, degree=63), MELO3C015414 (down-regulated, degree=53), MELO3C003487 (down-regulated, degree=51), MELO3C017200 (down-regulated, degree=51), MELO3C017059 (up-regulated, degree=51), MELO3C025274 (up-regulated, degree=49), MELO3C005479 (up-regulated, degree=43), MELO3C003101 (up-regulated, degree=42), MELO3C009486 (up-regulated, degree=42), and MELO3C017066 (up-regulated, degree=42).

Leaf colour mutants have been identified in many higher plants (Wan et al. 2015; Li et al. 2024; Li et al. 2025). However, there have been few reports on leaf colour mutants of *C. melo* and even fewer on the corresponding leaf colour genes (Zhao et al. 2019; Cao et al. 2023). In this study, a transcriptome sequence analysis showed that the DEGs identified from xantha mutant of *C. melo* in both the cotyledon and euphylla stages were significantly enriched in functions or pathways associated with photosynthesis (i.e., the MELO3C010813 (*ZAT10*) and MELO3C020718 (*MAPK3*) genes) and chloroplast development (i.e., the MELO3C026802 (*CRD1*) and MELO3C016714 (*PORA*) genes). Moreover, 18 common DEGs were identified to be TFs, including MELO3C005502, MELO3C005867, MELO3C006430, MELO3C012896, and MELO3C017940, which all belong to the ERF family. Notably, the identified photosynthesis-related gene MELO3C010813, which is also a transcription factor (TF), belongs to the ethylene response factor family. These findings merit further analysis.

Accumulating evidence has highlighted the fact that chlorophyll metabolism and chloroplast development affect the development of chlorotic leaves in crops. For example, the related genes *OsABCI7*and *OsHCF222* play important roles in chloroplast development in rice (Heet al. 2020), and *psbA, TOX* and *VDE* are also critical to the phenotype of albino tea (Du et al. 2009; Zeng et al. 2017). In all chloroplasts, the thylakoid membrane is interspersed with pigments, proteins, and other components that are essential to photosynthesis (Fitter 2002). It has been reported that the altered expression of many chloroplast and nuclear genes may affect the biogenesis of chloroplasts and subsequent chlorophyll metabolism, resulting in abnormal leaf colour (Yang et al. 2015; Huo et al. 2024). Other studies have also confirmed that the expression of genes related to chlorophyll biosynthesis and chloroplast development is consistently altered in leaf colour mutants (Wu et al. 2007; Su et al. 2012; Zhong et al. 2023). In this study, we also found that DEGs identified from xantha mutant of *C. melo* were enriched in functions or pathways associated with photosynthesis and chloroplast development, such as photosynthesis, light harvesting and reaction, plastid thylakoid membrane, plastid thylakoid, chloroplast thylakoid, and chloroplast thylakoid membrane. Therefore, we hypothesize that the dysregulation of photosynthesis and chloroplast development may be associated with the development of xantha mutant phenotypes.

Notably, based on the enriched GO function and KEGG

Table 2. The statistics of transcriptome sequencing for *C. melo* samples

TF ID	Family	Best hit in Arabidopsis thaliana	Blast e-value	Description for the best hit
MELO3C000922	NAC	AT2G43000.1	5.00E-37	NAC domain-containing protein 42
MELO3C009127	WRKY	AT2G38470.1	1.00E-43	WRKY DNA-binding protein 33
MELO3C009422	Trihelix	AT3G10040.1	1.00E-111	sequence-specific DNA binding transcription factors
MELO3C009859	Dof	AT5G39660.1	1.00E-110	cycling DOF factor 2
MELO3C010949	ZF-HD	AT1G75240.1	9.00E-69	homeobox protein 33
MELO3C015332	NF-YC	AT1G08970.3	4.00E-87	nuclear factor Y, subunit C9
MELO3C015488	bHLH	AT5G56960.1	1.00E-17	bHLH family protein
MELO3C020489	WRKY	AT2G38470.1	3.00E-44	WRKY DNA-binding protein 33
MELO3C023195	NAC	AT1G01720.1	3.00E-99	NAC family protein
MELO3C005502	ERF	AT4G17500.1	1.00E-83	ethylene responsive element binding factor 1
MELO3C005867	ERF	AT4G27950.1	3.00E-44	cytokinin response factor 4
MELO3C006430	ERF	AT3G23240.1	7.00E-76	ethylene response factor 1
MELO3C012896	ERF	AT3G23240.1	2.00E-61	ethylene response factor 1
MELO3C017940	ERF	AT1G72360.1	4.00E-23	ERF family protein
MELO3C009733	G2-like	AT3G10760.1	8.00E-95	G2-like family protein
MELO3C010813	C2H2	AT1G27730.1	4.00E-54	salt tolerance zinc finger
MELO3C016852	C3H	AT2G19810.1	1.00E-111	C3H family protein
MELO3C024332	C3H	AT1G04990.2	0.001	C3H family protein

pathway results, key DEGs, such as *ZAT10* and *MAPK3*, were identified as being associated with photosynthesis, and *CRD1* and *PORA* were associated with the development of chloroplasts. In particular, *ZAT10* was also identified as a transcription factor (TF). One study found that *ZAT10* can negatively regulate genes related to photosynthesis and carbohydrate metabolism, thereby playing a key role in photosynthesis (Maruyama et al. 2004). Lvet al. (2014) demonstrated that *SVR7* could participate in photo-oxidative stress responses in chloroplasts, possibly via the upregulation of *ZAT10*. Additionally, ZAT10 has been shown to play a role in regulating stress tolerance, particularly resistance to oxidative stress (Mittler et al. 2006; Dang et al. 2022). *ZAT10* is also implicated in the systemic acquired acclimation responses of leaves to high light levels, and its enhanced expression may result in the inhibition of photosynthesis (Rosselet al. 2007). These findings all reveal the involvement of *ZAT10* in the regulation of photosynthesis. Furthermore, *MAPK3* has been identified as an integrating stress signal that participates in stomatal development and subsequently influences photosynthesis (Geissler et al. 2013; Zhu et al. 2020). Given the key roles of *ZAT10* and *MAPK3* in photosynthesis, we hypothesize that the dysregulated of expression of *ZAT10* and *MAPK3* may be involved in xantha mutant phenotype formation via the regulation of photosynthesis. In addition, *CRD1* is localized to the chloroplast membranes. The *CRD1* gene encodes a putative di-iron enzyme that is required for photosystem I accumulation in copper- or oxygen-deficient cells in *Chlamydomonas reinhardtii* (Moseley et al. 2000). Moreover, *PORA* has been identified as one of the light-dependent protochlorophyllide-reducing enzymes that regulate chlorophyll biosynthesis in angiosperms (Reinbothe et al. 1996). Paddock et al. (2010) confirmed that *PORA* rescued bulk chlorophyll synthesis and normal development of the Arabidopsis porB-1 porC-1 mutant. Given the important roles of *CRD1* and *PORA* in chloroplast development, we hypothesize that the abnormal expression of *CRD1* and *PORA* may result in the formation of xantha mutant phenotypes via their effect on the development of chloroplasts.

Furthermore, a TF prediction analysis showed that 18 shared DEGs were TFs that belong to 11 TF families. Notably, MELO3C005502, MELO3C005867, MELO3C006430, MELO3C012896, and MELO3C017940 belong to the ERF family. Genes in the ERF family have been implicated in various physiological processes in plants (Nakano et al. 2006; Sheng et al. 2022). AP2/ERF transcription factors have been found to be involved in the response of tomato (*Solanum lycopersicum* L.) to tomato yellow leaf curly virus, including leaf curling and yellowing (Huang et al. 2016). An EAR-motif

that contains the ERF gene from tomato, *SlERF36*, has been shown to modulate photosynthesis and growth (Upadhyay et al. 2013). AP2/ERF gene from yellow leaf mutant Ginkgo biloba, was engaged in regulating pigment metabolism, and showed significantly different expression levels in the WT and YL (Sun et al. 2022). In addition, ERF genes have been found to function in light-induced anthocyanin production in *A. thaliana* leaves (Koyama and Sato, 2018). Anthocyanins have been identified as responsible for the red and blue colouration in many leaves, flowers, fruits, and seeds (Tian et al. 2011). These findings imply that the ERF TFs identified in this study may play a key role in the formation of xantha mutant phenotypes via the regulation of anthocyanin production.

In conclusion, our study revealed that the abnormal expression of *ZAT10*, *MAPK3*, *CRD1*, and PORA, as well as ERF TFs, is involved in the formation of the xantha mutant phenotype in *C. melo*, providing a fundamental understanding of the genetic causes of xantha phenotypes. The xantha phenotype formation of the mutant may be associated with the dysregulation of photosynthesis and the development of chloroplasts. However, no experimental validation was performed to verify the differential expression of key genes, which is a limitation of this study. Further research is still needed to verify our observations.

Supplementary material

Supplementary Fig. 1 is provided, that can be accessed at www.isgpb.org

Authors' contribution

Conceptualization of research (QS); Designing of the experiments (QS); Contribution of experimental materials (QS, NC); Execution of field/lab experiments and data collection (WZ, XZ); Analysis of data and interpretation (LL, WX, XL); Preparation of the manuscript (QS).

Acknowledgment

The authors express their gratitude to the National Natural Science Foundation of China (32160716, 32260776) for funding the research.

References

Altschul S.F., Madden T.L., Schäffer A.A., Zhang. J., Zhang Z., Wold B.J. and Pachter L. 1997. Gapped BLAST and PSI-BLAST: a new generation of protein database search programs. Nucleic Acids Res., **25**(17): 3389–3402. doi: 10.1093/nar/25.17.3389

Benjamini Y. and Hochberg Y. 1995. Controlling the false discovery rate: a practical and powerful approach to multiple testing. J. R. Statist. Soc. B, **57**(1): 289–300. doi:10.1111/j.2517-6161.1995.tb02031.x

Cao H., Li H., Lu L., Ji Y., Ma L., Li S. 2023. Screening and Validation of Internal Reference Genes for Quantitative Real-Time PCR Analysis of Leaf Colour Mutants in Dendrobium officinale. Genes (Basel)., **14**(5): 1112. doi: 10.3390/genes14051112.

Cai H., Chen H., Yi T., Daimon C.M., Boyle J.P., Peers C., Maudsley S. and Martin B. 2013. VennPlex--a novel Venn diagram program for comparing and visualizing datasets with differentially regulated datapoints. PLoS One, **8**(1): e53388. doi: 10.1371/journal.pone.0053388

Chen P., Hu H.T., Zhang Y., Wang Z.G., Dong G.J., Cui Y.T., Qian Q., Ren D.Y. and Guo L.B. 2018. Genetic analysis and fine-mapping of a new rice mutant, white and lesion mimic leaf. Plant Growth Regul., **85**: 425–435. doi: 10.1007/s10725-018-0403-7

Dang F., Li Y., Wang Y., Lin J., Du S., Liao X. 2022. *ZAT10* plays dual roles in cadmium uptake and detoxification in Arabidopsis. Front Plant Sci., **13**: 994100. doi: 10.3389/fpls.2022.994100.

Deng L.C., Qin P., Liu Z., Wang G.L., Chen W.L., Tong J.H., Xiao L.T., Tu B., Sun Y.T., Yan W., He H., Tan J., Chen X.W., Wang Y.P., Li S.G. and Ma B.T. 2017. Characterization and fine-mapping of a novel premature leaf senescence mutant yellow leaf and dwarf 1 in rice. Plant Physiol. Biochem., **111**: 50–58. doi: 10.1016/j.plaphy.2016.11.012

Du Y.Y., Shin S., Wang K.R., Lu J.L. and Liang Y.R. 2009. Effect of temperature on the expression of genes related to the accumulation of chlorophylls and carotenoids in albino tea. J. Hortic. Sci. Biotech., **84**(3): 365–369. doi:10.1080/14620316.2009.11512533

Fitter D.W., Martin D.J., Copley M.J., Scotland R.W. and Langdale J.A. 2002. GLK gene pairs regulate chloroplast development in diverse plant species. Plant J., **31**(6): 713–727. doi: 10.1046/j.1365-313x.2002.01390.x

Geissler N., Huchzermeyer B. and Koyro H.W. 2013. Effects of salt stress on photosynthesis under ambient and elevated atmospheric CO_2 concentration, p. 377-413. In: Ahmad P., Azooz M.M., Prasad M.N.V. (eds) Salt stress in plants. Springer, New York, NY. doi:10.1007/978-1-4614-6108-1_15

He Y., Shi Y., Zhang X., Xu X., Wang H., Li L., Zhang Z., Shang H., Wang Z., Wu J.L. 2020. The OsABCI7 Transporter Interacts with OsHCF222 to Stabilize the Thylakoid Membrane in Rice. Plant Physiol., **184**(1): 283-299. doi: 10.1104/pp.20.00445.

Huang B., Huang W., Liu Z., Peng Y., Qu Y., Zhou W., Huang J., Shu H., and Wen Q. 2024. Cytological, Physiological, and Transcriptome Analysis of Leaf-Yellowing Mutant in Camellia chekiangoleosa. Int. J. Mol. Sci., **26**(1):132. doi: 10.3390/ijms26010132.

Huang Y., Zhang B.L., Sun S., Xing G.M., Wang F., Li M.Y., Tian Y.S. and Xiong A.S. 2016. AP2/ERF transcription factors involved in response to tomato yellow leaf curly virus in tomato. Plant Genome, **9**(2): 1–15. doi: 10.3835/plantgenome2015.09.0082

Hu H.Z., Zhang R., Shang A.Q., Zhao L.J. and Zhi-Min A.L. 2007. Response of pigment content of golden-leaf plants to light intensity. Acta Horti. Sin., **34**: 717–722. https://www.ahs.ac.cn/EN/Y2007/V34/I3/717

Huo J., Zhang N., Gong Y., Bao Y, Li Y., Zhang L., Nie S. 2024. Effects of different light intensity on leaf colour changes in a Chinese cabbage yellow cotyledon mutant. Front Plant Sci., **15**: 1371451. doi: 10.3389/fpls.2024.1371451.

Kim D., Pertea G., Trapnell C., Pimentel H., Kelley R. and Salzberg S.L. 2013. TopHat2: accurate alignment of transcriptomes in the presence of insertions, deletions and gene fusions. Genome Biol., **14**(4): R36. doi: 10.1186/gb-2013-14-4-r36

Koyama T. and Sato F. 2018. The function of ETHYLENE RESPONSE FACTOR genes in the light-induced anthocyanin production of *Arabidopsis thaliana* leaves. Plant Biotechnol., **35**(1): 87–91. doi: 10.5511/plantbiotechnology.18.0122b

Leng N., Dawson J.A., Thomson J.A., Ruotti V., Rissman A.I., Smits

B.M., Haag J.D., Gould M.N., Stewart R.M. and Kendziorski C. 2013. EBSeq: an empirical Bayes hierarchical model for inference in RNA-seq experiments. Bioinformatics, **29**(8): 1035–1043. doi: 10.1093/bioinformatics/btt087

Li B., Zhang J., Tian P., Gao X., Song X., Pan X., Wu Y. 2024. Cytological, Physiological, and Transcriptomic Analyses of the Leaf Colour Mutant Yellow Leaf 20 (yl20) in Eggplant (*Solanum melongena* L.). Plants (Basel). 13(6):855. doi: 10.3390/plants13060855.

Li W., Li Q., Che J., Ren J., Wang A., Chen J. 2025. A Key R2R3-MYB Transcription Factor Activates Anthocyanin Biosynthesis and Leads to Leaf Reddening in Poplar Mutants. Plant Cell Environ. 48(3):2067-2082. doi: 10.1111/pce.15276.

Li Y., Zhang Z.Y, Wang P., Wang S.A., Ma L.L., Li L.F., Yang R.T., Ma Y.Z. and Wang Q. 2015. Comprehensive transcriptome analysis discovers novel candidate genes related to leaf colour in a *Lagerstroemia indica* yellow leaf mutant. Genes Genom, 37: 851–863.

Lv H.X., Huang C., Guo G.Q. and Yang Z.N. 2014. Roles of the nuclear-encoded chloroplast SMR domain-containing PPR protein SVR7 in photosynthesis and oxidative stress tolerance in *Arabidopsis*. J Plant Biol, 57(5): 291–301.
doi:10.1007/s12374-014-0041-1

Maruyama K., Sakuma Y., Meshi T., Iwabuchi M., Shinozaki K. and Yamaguchi-Shinozaki K. 2004. *Arabidopsis* cys2/his2-type zinc-finger proteins function as transcription repressors under drought, cold, and high-salinity stress conditions. Plant Physiol, 136(1): 2734–2746. doi: 10.1104/pp.104.046599

Ma X.Z., Sun X.Q., Li C.M., Huan R., Sun C.H., Wang Y., Xiao F.L., Wang Q., Chen P.R, Ma F.R., Zhang K., Wang P.R. and Deng X.J. 2017. Map-based cloning and characterization of the novel yellow-green leaf gene ys83 in rice (*Oryza sativa*). Plant Physiol Biochem, 111: 1–9. doi: 10.1016/j.plaphy.2016.11.007

Mittler R., Kim Y., Song L., Coutu J., Coutu A., Ciftci-Yilmaz S., Lee H., Stevenson B. and Zhu J.K. 2006. Gain- and loss-of-function mutations in Zat10 enhance the tolerance of plants to abiotic stress. Febs Lett, 580(28-29): 6537–6542. doi: 10.1016/j.febslet.2006.11.002

Moseley J., Quinn J., Eriksson M. and Merchant S. 2000. The Crd1 gene encodes a putative di-iron enzyme required for photosystem I accumulation in copper deficiency and hypoxia in *Chlamydomonas reinhardtii*. Embo J, 19(10): 2139–2151. doi: 10.1093/emboj/19.10.2139

Nakano T., Suzuki K., Fujimura T. and Shinshi H. 2006. Genome-wide analysis of the ERF gene family in *Arabidopsis* and rice. Plant Physiol, 140(2): 411–432. doi: 10.1104/pp.105.073783

Paddock T.N., Mason M.E., Lima D.F. and Armstrong G.A. 2010. *Arabidopsis* protochlorophyllide oxidoreductase A (PORA) restores bulk chlorophyll synthesis and normal development to a porB porC double mutant. Plant Mol Biol, 72(s4-5): 445–457. doi: 10.1007/s11103-009-9582-y

Peng Y., Jiang Y., Chen Q., Lin Y., Li M., Zhang Y., Wang Y., He W., Zhang Y., Wang X., Tang H., Luo Y. 2025. Comparative transcriptome and metabolomic analysis reveal key genes and mechanisms responsible for the dark-green leaf colour of a strawberry mutant. Plant Physiol Biochem. 218:109327. doi:10.1016/j.plaphy.2024.109327.

Reinbothe S., Reinbothe C., Lebedev N. and Apel K. 1996. *PORA* and *PORB*, two light-dependent protochlorophyllide-reducing enzymes of angiosperm chlorophyll biosynthesis. Plant Cell, 8(5): 763–769. doi: 10.1105/tpc.8.5.763

Rossel J.B., Wilson P.B., Hussain D., Woo N.S., Gordon M.J., Mewett O.P., Howell K.A., Whelan J., Kazan K. and Pogson B.J. 2007. Systemic and intracellular responses to photooxidative stress in *Arabidopsis*. Plant Cell, 19(12): 4091–4110. doi: 10.1105/tpc.106.045898

Shannon P., Markiel A., Ozier O., Baliga N.S., Wang J.T., Ramage D., Amin N., Schwikowski B. and Ideker T. 2003. Cytoscape: a software environment for integrated models of biomolecular interaction networks. Genome Res, 13(11): 2498–2504. doi: 10.1101/gr.1239303

Shao Q. and Yu Z.Y. 2013. Physiological and biochemical characterization of Xantha mutant of *Cucumis melo* L. Res J Biotechnol, 8(5): 72–77.

Sheng S., Guo X., Wu C., Xiang Y., Duan S., Yang W., Li W., Cao F., Liu L. 2022. Genome-wide identification and expression analysis of DREB genes in alfalfa (Medicago sativa) in response to cold stress. Plant Signal Behav. 17(1):2081420. doi: 10.1080/15592324.2022.2081420.

Su N., Hu M.L., Wu D.X., Wu F.Q., Fei G.L., Lan Y., Chen X.L., Shu X.L., Zhang X., et al. (2012) Disruption of a rice pentatricopeptide repeat protein causes a seedling-specific albino phenotype and its utilization to enhance seed purity in hybrid rice production. Plant Physiol, 159(1): 227–238. doi: 10.1104/pp.112.195081

Sun Y., Bai P.P., Gu K.J., Yang S.Z., Lin H.Y., Shi C.G., Zhao Y.P. 2022. Dynamic transcriptome and network-based analysis of yellow leaf mutant Ginkgo biloba. BMC Plant Biol. 22(1):465. doi: 10.1186/s12870-022-03854-9.

Szklarczyk D., Morris J.H., Cook H., Kuhn M., Wyder S., Simonovic M., Santos A., Doncheva N.T., Roth A., Bork P., Jensen L.J. and von Mering C. 2017. The STRING database in 2017: quality-controlled protein–protein association networks, made broadly accessible. Nucleic Acids Res, 45(D1): D362–D368. doi: 10.1093/nar/gkw937

Tanaka A., and Tanaka R. 2006. Chlorophyll metabolism. Curr Opin Plant Biol, 9(3): 248–255. doi:10.1016/j.pbi.2006.03.011

Tian J., Shen H., Zhang J., Song T. and Yao Y. 2011. Characteristics of chalcone synthase promoters from different leaf-colour Malus crabapple cultivars. Sci Hortic-Amesterd, 129(3): 449–458. doi: 10.1038/hortres.2017.70

Trapnell C., Williams B.A., Pertea G., Mortazavi A., Kwan G., van Baren M.J., Salzberg S.L., Wold B.J. and Pachter L. 2010. Transcript assembly and quantification by RNA-Seq reveals unannotated transcripts and isoform switching during cell differentiation. Nat biotechnol, 28(5): 511–515. doi: 10.1038/nbt.1621

Upadhyay R.K., Soni D.K., Singh R., Dwivedi U.N., Pathre U.V., Nath P. and Sane A.P. 2013. SlERF36, an EAR-motif-containing ERF gene from tomato, alters stomatal density and modulates photosynthesis and growth. J Exp Bot, 64(11): 3237–3247. doi: 10.1093/jxb/ert162

Wan C.M., Li C.M., Ma X.Z., Wang Y., Sun C.H., Huang R., Zhong P., Gao Z.Y., Chen D., Xu Z., Zhu J., Gao X., Wang P. and Deng X. 2015. GRY79 encoding a putative metallo-β-lactamase-trihelix chimera is involved in chloroplast development at early seedling stage of rice. Plant Cell Rep, 34(8): 1353–1363. doi: 10.1007/s00299-015-1792-y

Wang Z., Xu H., Wang F., Sun L., Meng X., Li Z., Xie C., Jiang H., Ding G., Hu X., Gao Y., Qin R., Zhao C., Sun H., Cui F., and Wu Y. 2024. EMS-induced missense mutation in TaCHLI-7D affects leaf

colour and yield-related traits in wheat. Theor Appl Genet. 137(10):223. doi: 10.1007/s00122-024-04740-8.

Wu H.Y., Shi N.R., An X.Y., Liu C., Fu H.F., Cao L., Feng Y., Sun D.J. and Zhang L.L. 2018. Candidate genes for yellow leaf colour in common wheat (*Triticum aestivum* L.) and major related metabolic pathways according to transcriptome profiling. Int. J. Mol. Sci., **19**(6): 1594. doi: 10.3390/ijms19061594

Wu Z.M., Zhang X., He B., Diao L.P., Sheng S.L., Wang J.L., Guo X.P., Su N., Wang L.F., Jiang L., Wang C., Zhai H. and Wan J. 2007. A chlorophyll-deficient rice mutant with impaired chlorophyllide esterification in chlorophyll biosynthesis. Plant Physiol., **145**(1): 29–40. doi: 10.1104/pp.107.100321

Yang D.L., Li S., Li M.F., Yang X.L., Wang W.T., Cao Z.Y. and Li W. 2012. Physiological characteristics and leaf ultrastructure of a novel chlorophyll-deficient chd6 mutant of *vitis venifera* cultured in vitro. J. Plant Growth Reg., **31**(1): 124–135. doi:10.1007/s00344-011-9225-9

Yang Y.X., Chen X.X., Xu B., Li Y.X., Ma Y.H. and Wang G.D. 2015. Phenotype and transcriptome analysis reveals chloroplast development and pigment biosynthesis together influenced the leaf colour formation in mutants of *Anthurium andraeanum* 'Sonate'. Front Plant Sci., **6**: 139. doi:10.3389/fpls.2015.00139

Yuan G.S., Li Y.C., Chen. B.F, He H., Wang Z.Y., Shi J.H., Yang Y., Zou C.Y. and Pan G.T. 2021. Identification and fine mapping of a recessive gene controlling zebra leaf phenotype in maize. Mol. Breeding, **41**(2): 1–13.

Yu G., Wang L.G., Han Y. and He Q.Y. 2012. clusterProfiler: an R package for comparing biological themes among gene clusters. Omics, **16**(5): 284–287. doi:10.1089/omi.2011.0118

Zeng X.Y., Tang R., Guo H.R., Ke S.H., Teng B., Hung Y.H., Xu Z., Xie X.M., Hsieh T.F. and Zhang X.Q. 2017. A naturally occurring conditional albino mutant in rice caused by defects in the plastid-localized OsABCI8 transporter. Plant Mol. Biol., **94**(1-2): 137–148. doi:10.1007/s11103-017-0598-4

Zhang H., Li J., Yoo J.H., Yoo S.C., Cho S.H., Koh H.J., Seo H.S. and Paek N.C. 2006. Rice Chlorina-1 and Chlorina-9 encode ChlD and ChlI subunits of Mg-chelatase, a key enzyme for chlorophyll synthesis and chloroplast development. Plant Mol. Biol., **62**(3): 325–337. doi:10.1007/S11103-006-9024-Z

Zhao C.M., Cui J.Z., Li X.G., Chen B.J. and Yu Z.Y. 2019. Proteomic analysis of chloroplasts from chlorophyll-deficient melon mutant. Photosynthetica, **57**(3): 866–874. doi:10.32615/ps.2019.078

Zhong S., Yang H., Chen C., Ren T., Li Z., Tan F. and Luo P. 2023. Phenotypic characterization of the wheat temperature-sensitive leaf colour mutant and physical mapping of mutant gene by reduced-representation sequencing. Plant Sci., **330**: 111657. doi: 10.1016/j.plantsci.

Zhu X., Zhang N., Liu X., Wang S., Li S., Yang J., Wang F. and Si H. 2020. *StMAPK3* controls oxidase activity, photosynthesis and stomatal aperture under salinity and osmosis stress in potato. Plant Physiol. Biochem., **156**: 167-177. doi: 10.1016/j.plaphy.2020.09.012.

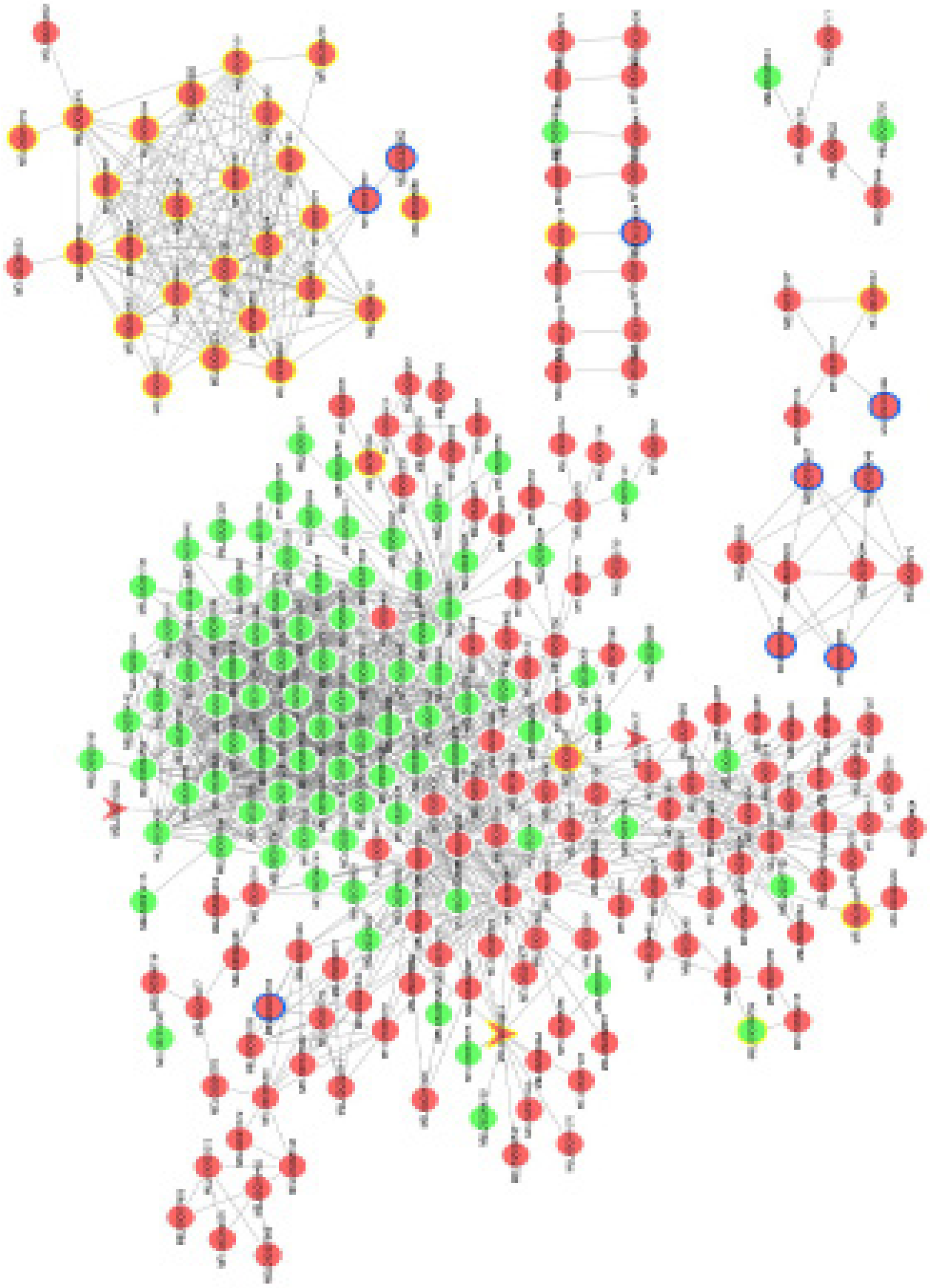

Supplementary Fig. 1. Figure depecting differentially expressed genes containing nodes and edges